Article

Lanthanide-Containing Polymer Nanoparticles for Biological Tagging Applications: Nonspecific Endocytosis and Cell Adhesion

Cdric Vancaeyzeele, Olga Ornatsky, Vladimir Baranov, Lei Shen, Ahmed Abdelrahman, and Mitchell A. Winnik

J. Am. Chem. Soc., **2007**, 129 (44), 13653-13660• DOI: 10.1021/ja073970w • Publication Date (Web): 12 October 2007

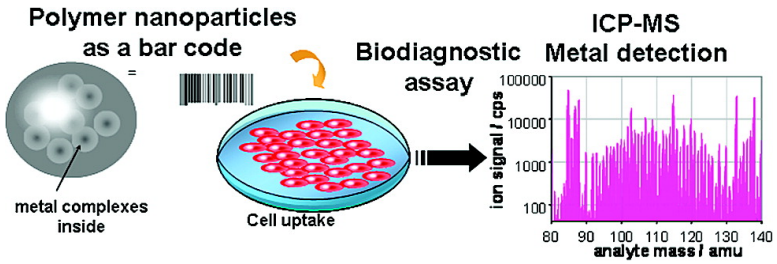

More About This Article

Additional resources and features associated with this article are available within the HTML version:

- Supporting Information
- Links to the 1 articles that cite this article, as of the time of this article download
- Access to high resolution figures
- Links to articles and content related to this article
- Copyright permission to reproduce figures and/or text from this article

View the Full Text HTML

J|A|C|S
ARTICLES
Published on Web 10/12/2007

Lanthanide-Containing Polymer Nanoparticles for Biological Tagging Applications: Nonspecific Endocytosis and Cell Adhesion

Cédric Vancaeyzeele,§ Olga Ornatsky, Vladimir Baranov, Lei Shen, Ahmed Abdelrahman, and Mitchell A. Winnik*

Contribution from the Department of Chemistry, University of Toronto, 80 St. George Street, Toronto, Ontario, Canada M5S 3H6, and Institute of Biomaterials and Biomedical Engineering, University of Toronto, 164 College Street, Room 407, Toronto, Ontario, Canada M5S 3G9

Received June 14, 2007; E-mail: mwinnik@chem.utoronto.ca

Abstract: We describe the synthesis and characterization of element-encoded polystyrene nanoparticles with diameters on the order of 100 nm and a narrow size distribution. Individual particles contain ca. 10^3 chelated lanthanide ions, of either a single element or a mixture of elements. These particles were effectively internalized by nonspecific endocytosis into three cell lines associated with human leukemia. Using an assay based upon ICP-MS detection, we could monitor quantitatively cell adhesion induced by cell differentiation of THP-1 cells in response to phorbol ester stimulation (PMA) in single cell type or mixed cultures.

1. Introduction

Many biodiagnostic assays require tags bearing bar codes that can serve to identify the tagged species. In current technology, these markers are often combinations of organic dyes and/or quantum dots, whose identity is revealed by their photoluminescence. One of the limitations of this technique is the number of different dyes and different emission intensities that can be read simultaneously, i.e., the information content of the bar code. A much larger amount of information can be coded if one employs different metal atoms and isotopes as labels. The type of metal present and the amount can be measured with high sensitivity by inductively coupled plasma mass spectrometry (ICP-MS).[1] This technique has unit mass resolution and a linear dynamic range extending over 8 orders of magnitude. To be useful for biological assays, the metals that one employs should have low natural abundance. From this perspective, the lanthanides are particularly useful. This family of elements not only has a similar chemistry but also represents 24 elements and 54 individual stable isotopes.

There are a number of different ways in which one can imagine tagging cells or biological macromolecules with lanthanide (Ln) atoms or ions. For example, several lanthanide-containing labeling agents are commercially available for biodiagnostic assays. These, however, are designed to take advantage of the photoluminescent properties of certain ions. For effective bar codes and enhanced sensitivity, tags containing a much larger number of ions per tag are needed. Here one can imagine metal chelating polymeric tags, containing significant numbers of a given ion bound to each chain. Alternatively, one might employ polymer or inorganic nanoparticles bearing upward of 10^3 lanthanide ions per nanoparticle. In this paper, we describe the synthesis and characterization of a series of polystyrene nanoparticles containing approximately 2000 Ln ions per particle. This approach allows one to synthesize particles containing either a single type of ion or a mixture of different lanthanide ions. The basic design strategy involves miniemulsion polymerization of styrene in the presence of Ln ions bound to an organic ligand (tris-4,4,4-trifluoro-1-(2-naphthyl-1,3-butanedione)) that renders the complex electrically neutral and soluble in organic solvents such as styrene. We then test the utility of these particles as tags for cell-based assays in the study of three different human leukemia cell lines.

Cell-based assays have become invaluable tools in the screening of potential drug candidates and bioactive compounds, from library mining and lead optimization to target validation, and in basic research applications. The aim of a cell-based assay is to evaluate cellular response to biochemical challenges in an environment which closely mimics the in vivo conditions. Traditionally, multiwell microtiter plates are used to perform a large number of parallel experiments with several cell lines simultaneously, with each cell type in a separate well undergoing the same experimental stimulation. However, this approach is limited to the investigation of same cell−cell and cell-to-matrix interactions.

Simple yet accurate methods that allow monitoring of complex heterogeneous cell population responses comparable to living tissue are currently poorly developed. One possible explanation is that the conventional fluorescent cell tagging methods[2] are difficult to multiplex due to the intrinsic physical properties of fluorophors, organic dyes with a narrow excitation spectrum, precluding simultaneous excitation of many different

§ Current address: Université de Cergy-Pontoise, Laboratoire de Physicochimie des Polymères et des Interfaces (LPPI), 95031 Cergy-Pontoise, Cedex, France.

(1) Baranov, V. I.; Quinn, Z.; Bandura, D. R.; Tanner, S. D. *Anal. Chem.* **2002**, *74* (7), 1629−1636.

dyes, and wide emission spectrum creating an overlap between different detection channels and low dynamic range. These factors make quantification of the relative amounts of the fluorochromes in cells difficult.[3] Although novel microsphere encoding technologies using optical signatures of fluorescent microbeads (for example, Fluoresbrite, Polysciences Inc.) and semiconductor nanocrystals (Qdot, Quantum Dot Corp) incorporated into polystyrene beads, as well as graphically and electronically encoded beads, have advantages over fluorescent dyes, there remain numerous disadvantages described in detail in the review paper by Braeckmans et al.[4]

Examples of labeling cells with encoded microspheres include transplantation, migration, and adhesion studies with fluorescent beads that enable cell type identification and analysis of graft migration in the host over extended time periods, research on pulmonary blood flow and blood-barrier function, cell adhesion to synthetic matrices, and phagocytosis in vitro.[5,6]

In the present paper, we demonstrate a novel microbead encoding method employing lanthanides and ICP-MS detection.[7,8] It is expected that many thousands of distinguishable analytical beads can be produced by the incorporation of various concentrations and ratios of metals. A clear advantage of this technique is the large number of uniquely encoded beads. Theoretically, combinations of five-element labels can generate tens of thousands of microbead signatures. Furthermore, the beads can be functionalized to bind bioactive compounds such as cytokines, growth factors, or small molecules, which will make the microbeads operate as delivery vehicles, as well as tagging reagents for cell-based assays.

We show how cell adhesion[9] following chemically induced cellular differentiation can be quantified in a robust manner via an ICP-MS assay.[1] The assay takes advantage of nonspecific endocytosis of the polymer nanoparticles[10] by the cells. This methodology offers significant advantages over traditional assays of cell adhesion based upon correlation of fluorescence intensity with cell numbers.[11]

2. Experimental Section

2.1. Instrumentation. High-resolution mass spectra were obtained using a VG 70-250S (double focusing) mass spectrometer at 70 eV. The particle diameters and particle diameter dispersities were measured by dynamic light scattering (DLS) both with a BI90 particle sizer (Brookhaven Instruments Corporation) at a fixed scattering angle of 90° and with a wide angle light scattering photometer from ALV. The light source was a JDS Uniphase He−Ne laser ($\lambda_0 = 632.8$ nm, 35 mW) emitting vertically polarized light. The scattered light was detected by a Dual ALV-High Q.E. APD avalanche photodiode module. This detector was interfaced to the ALV-5000/EPP multiple time delay digital correlator with 288 exponentially spaced channels that measured the correlation function in real time. All measurements were carried out at a scattering angle of 90°. Zeta potentials were determined on 10.0 mL samples in unbuffered water at 25 °C using a Malvern Instruments 3000HS Zetasizer. Values were calculated from the average of five separate runs on the same sample.

Typical operating conditions[1] of the ICP-MS instrument ELAN DRCPlus (Perkin-Elmer SCIEX) are based on stable Ar plasma optimized to provide a <3% CeO^+/Ce^+ ratio in 1 ppb standard multielement solution diluted in 10% HCl. The requirement was achieved applying 1400 W forward plasma power, 17 L/min Ar plasma gas flow, 1.2 L/min auxiliary Ar flow, and 0.95 L/min nebulizer (Burgener Micromist) Ar flow. Under these operating conditions typical sensitivity is 4×10^4 cps for 1 ppb Ir standard solution in 10% HCl. This instrument has single mass resolution for signal intensities in adjacent channels that do not differ by more than 10^6. The detection limits for lanthanide elements are less that 1 ppb. The elemental analysis of samples containing high concentrations of HCl, digested cells, submicron beads, and buffers containing high concentrations of dissolved solids is not routine. The challenge comes from the effect of possible matrix suppression of analyte signals by dominant ions and interferences by polyatomic species. These effects, including isotope abundances and polyatomic ions (oxides, hydroxides, nitrides, and carbides, for which the ratio is invariant for a given plasma condition and typically are of the order of 0.01% to 1% of the dominant signal), were investigated independently. The results of this investigation, which are of particular interest to the analytical chemistry community, will be published elsewhere. The main conclusion is that these matrix effects introduce errors that are smaller than the differences in replicate measurements.

The sample uptake rate was adjusted depending on the particular experiment and sample size, typically 100 μL/min. A MicroFlow PFA-ST concentric nebulizer (Elemental Scientific, Inc) was used in all instances. Experiments were performed using an autosampler (Perkin-Elmer AS 91) modified for operation with Eppendorf 1.5 mL tubes. Sample size varied from 150 to 300 μL. Standards were prepared from 1000 μg/mL PE Pure Single-Element Standard solutions (Perkin-Elmer, Shelton, CT) by sequential dilution with high-purity deionized water (DIW) produced using an Elix/Gradient (Millipore, Bedford, MA) water purification system.

The composition of selected lanthanide-containing polymer nanoparticles was also analyzed by ICP-atomic emission spectroscopy (ICP-AES) employing an Optima 3000 DV instrument equipped with an AS-90 autosampler. To prepare these samples for ICP-AES and ICP-MS analysis, we employed two different methods, and a specific example is given for the CV97 polymer beads. In the first method, triplicate samples of CV97 bead solution (0.15 mL, 1:11 volume ratio diluted from the original, solids content 0.0173 g/mL) were mixed with aqua regia (HCl/HNO_3, v/v = 3:1, 2.0 mL) and heated to 80 °C for 3 h until a clear solution was attained. Then the solution was diluted to 3.0 mL with DI water for ICP-AES and ICP-MS analysis. In the second (direct injection) method, triplicate samples of the same CV97 bead solution (solids content 0.0173 g/mL) were diluted with DI water to 3.0 mL and directly subjected to ICP-AES and ICP-MS analysis. The ICP-AES was also calibrated with the single element standard solutions described above.

2.2. Materials. 4,4,4-Trifluoro-1-(2-naphthyl-1,3-butanedione) (Aldrich), lanthanum(III) chloride hydrate (Fluka), praseodymium(III)

(2) (a) Molday, R. S.; Dreyer, W. J.; Rembaum, A.; Yen, S. P. S. *J. Cell Biol.* **1975**, *64*, 75−88. (b) Park, J. Y.; Arnaout, M. A.; Gupta, V. *J. Biomol. Screen.* **2007**, *12*, 406−17.
(3) Gratama, J. W.; D'hautcourt, J. L.; Mandy, F.; Rothe, G.; Barnett, D.; Janossy, G.; Papa, S.; Schmitz, G.; Lenkei, R. *Cytometry* **1998**, *33*, 166−78.
(4) Braeckmans, K.; De Smedt, S. C.; Leblans, M.; Pauwels, R.; Demeester, J. *Nat. Rev. Drug Discovery* **2002**, *1*, 447−56.
(5) (a) De, V. G.; Haseldonckx, M.; Flameng, W.; Borgers, M.; Reneman, R. S.; van, R. K. *J. Neurosci. Methods* **2003**, *122*, 149−56. (b) Geijtenbeek, T. B. H.; van Kooyk, Y.; van Vliet, S. J.; Renes, M. H.; Raymakers, R. A. P.; Figdor, C. G. *Blood* **1999**, *94*, 754−64. (c) Molema, G.; Mesander, G.; Kroesen, B. J.; Helfrich, W.; Meijer, D. K.; de Leij, L. F. *Cytometry* **1998**, *32*, 37−43.
(6) (a) Satoh, A.; Huard, J.; Labrecque, C.; Tremblay, J. P. *J. Histochem. Cytochem.* **1993**, *41*, 1579−82. (b) Schimmel, C.; Frazer, D.; Glenny, R. W. *Am. J. Physiol. Heart Circ. Physiol.* **2001**, *280*, H2496−H2506. (c) Van Oosterhout, M. F.; Prinzen, F. W.; Sakurada, S.; Glenny, R. W.; Hales, J. R. *Am. J. Physiol.* **1998**, *275*, H110−H115. (d) Winter, S. S.; Sweatman, J. J.; Larson, R. S. *Cytometry* **2000**, *40*, 26−31.
(7) Baranov, V. I.; Quinn, Z. A.; Bandura, D. R.; Tanner, S. D. *J. Anal. At. Spectrom.* **2002**, *17*, 1148−52.
(8) Tanner, S. D.; Ornatsky, O.; Bandura, D. R.; Baranov, V. I. *Spectrochim. Acta, Part B* **2007**, *62*, 188−95.
(9) Christofori, G. *Nature* **2006**, *441* (7092), 444−450.
(10) Holzapfel, V.; Musyanovych, A.; Landfester, K.; Lorenz, M. R.; Mailander, V. *Macromol. Chem. Phys.* **2005**, *206* (24), 2440−2449.
(11) Brautboucher, F.; Pichon, J.; Rat, P.; Adolphe, M.; Aubery, M.; Font, J. *J. Immunol. Methods* **1995**, *178* (1), 41−51.

Table 1. Reactants for the Miniemulsion Polymerizations,[a,b] as well as Selected Characteristics of the Particles

sample name	LM (mg)	SDS (mg)	INI (mg)	Ln complex added (mg/g of styrene)	Ln complex measured (mg/g of styrene)[c,d]	R_h (nm)[e] z-average	R_h (nm) number average	PDI[e]	zeta potential[f]
CV28	120	150	K (60)	--	--	61		0.07	-58.7 ± 0.3
CV64	120	120	K (60)	--	--	62		0.02	--
CV70	120	150	A (60)	--	--	68		0.08	-56.9 ± 0.2
CV40	120	300	K (60)	Ho (42)		51	27.5	0.209	-43.0 ± 1.6
CV45	120	300	K (60)	Tb (46)		36		0.03	-39.2 ± 1.0
CV74	120	150	A (60)	Eu (25)	Eu (14.6)	88	82	0.038	-30.0 ± 1.2
CV90	120	150	K (960)	Pr, Ho, La, Tb, Eu (25 each)		77		0.03	-41.1 ± 1.2
CV97	120	150	K (60)	Pr (12.5), Ho (12.5), Tb (12.5), Eu (25)	Pr (2.3), Ho (2.7), Tb (2.7), Eu (6.1)	45	39	0.030	-45.9 ± 3.6

[a] All reactions contained 6.0 g of styrene, 60 mg of DVB, 27.0 g of deionized water, and 0.15 g of $NaHCO_3$. [b] Abbreviations: S,: styrene; LM, lauryl methacrylate; SDS, sodium dodecyl sulfate; INI, initiators: K, potassium persulfate (KPS); A, 2,2′-azobis(2-methylbutyronitrile) (AMBN); DVB, divinylbenzene. [c] As measured by ICP-AES and/or ICP-MS as discussed in the text. [d] The element content in atoms per bead, calculated using a particle diameter d = twice the number average value of R_h: CV74, Eu (2300); CV97, Pr (380), Ho (550), Tb (460), Eu (1000). [e] PDI values were obtained with the BI90 particle sizer. Number-average R_h values were obtained from analysis of right-angle DLS data obtained with the ALV instrument. Both instruments gave very similar values of the *z*-average R_h. [f] Average of 5 runs $\pm$ 1 standard deviation.

chloride hexahydrate (Aldrich), europium(III) chloride hexahydrate (Aldrich), terbium(III) chloride hexahydrate (Aldrich), Holmium(III) chloride hexahydrate (Aldrich), and ammonium hydroxide (NH_3 30% in water) (Fisher Scientific) were used as received. Water was deionized through a MilliQ purification system and used in all synthetic and biological experiments. Styrene (Aldrich) was distilled before use. Dichloromethane (CH_2Cl_2) was distilled from calcium hydride before use. Divinylbenzene (DVB, Aldrich), lauryl methacrylate (Aldrich), methacrylic acid (Aldrich), sodium dodecyl sulfate (SDS, Aldrich), sodium bicarbonate ($NaHCO_3$, Aldrich), potassium persulfate (KPS or $K_2S_2O_8$, Aldrich), and 2,2′-azobis (2-methylbutyronitrile) (AMBN, Wako) were used as received. Phorbol 12-myristate 13 acetate (PMA) (Sigma) was dissolved in DMSO at 10 μg/mL as stock solution and kept frozen.

2.3. Synthesis of the Lanthanide Complexes. These syntheses follow the procedure described by Melby et al.[12] A detailed example is given for europium(III) tris(4,4,4-trifluoro-1-(2-naphthyl-1,3-butanedione)): 4,4,4-trifluoro-1-(2-naphthyl-1,3-butanedione) (0.8 g, 3 mmol) was dissolved in a mixture of ethanol (75 mL) and ammonium hydroxide (19 mL, 0.3 mol) under vigorous stirring at room temperature. As soon as a yellowish transparent solution was obtained, a solution of europium(III) chloride (0.366 g, 1 mmol) dissolved in deionized water (10 mL) was added dropwise. The complex instantaneously precipitated. The mixture was kept under stirring for 12 h. Then, the product was extracted in CH_2Cl_2 (50 mL). The organic phase was washed three times with deionized water (50 mL) and dried over $MgSO_4$. After filtration, the solvent was evaporated, and a yellow solid was obtained. It was dried in a vacuum oven. (Weight: 2.75 g, Yield: 95%, LRMS (EI, *m*/*z*) calcd for $C_{42}H_{18}F_9O_6Eu$ (M^+) 947.62, found 947.57).

A similar procedure was used to synthesize the other lanthanide complexes: lanthanum tris-4,4,4-trifluoro-1-(2-naphthyl-1,3-butanedione) (1.70 g, yield: 90%, LRMS (EI, *m*/*z*) calcd for $C_{42}H_{18}F_9O_6La$ (M^+) 934.56, found 934.54), praseodymium tris-4,4,4-trifluoro-1-(2-naphthyl-1,3-butanedione) (3.48 g, yield: 93%, LRMS (EI, *m*/*z*) calcd for $C_{42}H_{18}F_9O_6Pr$ (M^+) 936.57, found 936.54), neodymium tris-4,4,4-trifluoro-1-(2-naphthyl-1,3-butanedione) (1.46, yield: 78%, LRMS (EI, *m*/*z*) calcd for $C_{42}H_{18}F_9O_6Nd$ (M^+) 939.90, found 939.84), samarium tris-4,4,4-trifluoro-1-(2-naphthyl-1,3-butanedione) (3.71 g, yield: 98%, LRMS (EI, *m*/*z*) calcd for $C_{42}H_{18}F_9O_6Sm$ (M^+) 946.02, found 946.04), terbium tris-4,4,4-trifluoro-1-(2-naphthyl-1,3-butanedione) (3.56 g, yield: 93%, LRMS (EI, *m*/*z*) calcd for $C_{42}H_{18}F_9O_6Tb$ (M^+) 954.58, found 954.20), dysprosium tris-4,4,4-trifluoro-1-(2-naphthyl-1,3-butanedione) (1.83 g, yield: 96%, LRMS (EI, *m*/*z*) calcd for $C_{42}H_{18}F_9O_6Dy$ (M^+) 958.16, found 958.12) and holmium tris-4,4,4-trifluoro-1-(2-naphthyl-1,3-butanedione) (2.96 g, yield: 77%, LRMS (EI, *m*/*z*) calcd for $C_{42}H_{18}F_9O_6Ho$ (M^+) 960.59, found 960.56).

2.4. Synthesis of Lanthanide-Containing Polystyrene Particles by Miniemulsion Polymerization. The reactants for the miniemulsion polymerization are listed in Table 1. In a typical reaction, up to 50 mg of a lanthanide complex or 125 mg of a mixture of lanthanide complexes were dissolved in a mixture of styrene (6 g), divinylbenzene (DVB, 60 mg, 4.6×10^{-4} mol) (1 wt % based on styrene), and lauryl methacrylate (120 mg, 4.6×10^{-4} mol) (2 wt % based on styrene). As soon as the complexes were dissolved, this homogeneous phase was mixed with the aqueous phase composed of deionized water (27 g), sodium dodecyl sulfate (SDS, 0.30 g, 1.0 mmol) (5 wt % based on styrene), and sodium bicarbonate ($NaHCO_3$,0.15 g, 1.8 mmol). The mixture was emulsified under magnetic stirring for 15 min, and then the miniemulsion was prepared by ultrasonication with a Branson Digital sonifier model 450 at 60% amplitude for 4 min (1 s pulse on, 2 s pulse off). During this step the mixture was cooled with ice. Then, the miniemulsion was transferred to a three-neck flask reactor equipped with a condenser and stirred mechanically. The reaction mixture was heated to 70 °C, initiated by the addition of potassium persulfate (KPS) (60 mg, 0.22 mmol) in water (3 mL). The reaction mixture was heated with stirring for 6 h at 70 °C and then allowed to cool to room temperature. A stable coagulum-free latex dispersion was obtained (ca. 36 mL, 16.6 wt % solids) and was stored at room temperature. For example, the dispersion of particles containing the terbium complex (46 mg/g of styrene) (CV40) had a narrow size distribution (PDI = 0.03) and a mean diameter $d_m = 71$ nm as measured by the BI90 particle sizer (cf. Table 1).

Polymer nanoparticles employed in bioassays were diluted 1:10 in Milli-Q H_2O and sterilized by pasteurization (24 h 70 °C).

2.4.1. Miniemulsion Polymerization with an Oil-Soluble Initiator. One sample (CV74) was synthesized using 2,2′-azobis (2-methylbutyronitrile) (AMBN), an oil soluble initiator. To obtain colloidally stable particles, methacrylic acid was added to the recipe (Table 1). The reactions were carried out as described above.

2.4.2. "Core−Shell" Particles by Seeded Emulsion Polymerization. Without further purification, a diluted aliquot of CV97 (13.0 mL, 3.8% solids) was placed under a nitrogen atmosphere in a three-neck flask reactor equipped with a condenser and stirred mechanically. The reactants for the second stage [water (5.0 mL), SDS (25 mg), $NaHCO_3$ (50 mg), KPS (68 mg), styrene (4.75 g), divinylbenzene (50 mg), and methacrylic acid (250 mg)] were combined in a 25 mL Erlenmeyer flask, emulsified under magnetic stirring, and then were introduced as an emulsion dropwise via a feeding pump (Model QSY from Fluid Metering Inc., 0.02 mL/min) into the solution of the seed particles

(12) Melby, L. R.; Abramson, E.; Caris, J. C.; Rose, N. J. *J. Am. Chem. Soc.* **1964**, *86* (23), 5117−5125.

Chart 1. Ligand, **1**; Lanthanide Complex, **2**

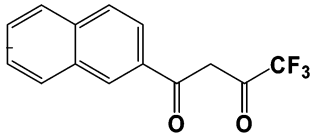

1

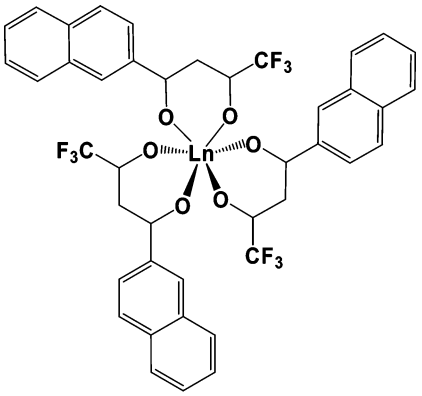

2

heated to 70 °C. A stable coagulum-free latex suspension (around 25 mL, 22 wt % solids) was obtained. The particles obtained (CV98) had a *z*-averaged R_h = 70 nm with a PDI = 0.09.

2.5. Tests of Colloidal Stability and Cation Release into the Aqueous Phase. The colloidal stability as a function of pH at room temperature of a sample of multielement lanthanide-loaded particles CV90 (d_z = 134 nm; Ho, Tb, La, Pr, and Eu complexes) was compared with that of a metal-free particle sample CV64 (d_z = 104 nm). These samples were first diluted 5× with water. The two diluted latexes were stable at pH = 9. Five samples were prepared in different vials. The pH of these latexes was slowly decreased by addition of HCl (0.1 M). The onset of flocculation turbidity was determined visually.

In order to determine if there was any lanthanide cation release from the polystyrene particles, the water phase (serum) was analyzed by ICP-MS. An aliquot of the latex was allowed to stir at pH 9 for 72 h. Then particle flocculation was promoted by addition of 1 g of solid NaCl to the mixture under stirring. The solid was allowed to settle for 12 h. Afterward, the mixture was passed through an inorganic membrane filter (Anotop 25, 0.2 μm, Whatman). By ICP-MS, the count rate detected in the supernatant (100 to 300 ppb for ^{159}Tb, ^{153}Eu, ^{139}La, ^{165}Ho, ^{141}P) was comparable to that detected in deionized water as a reference. The clear supernatant also gave no detectable counts using the BI90 particle sizer, implying the absence of any colloidal material.

2.6. Cell Lines. KG-1a, human acute myelogenous leukemia, and THP-1, a human acute monocytic leukemia, as well as K562, chronic myeloid leukemia cell lines were purchased from ATCC (Manassas, VA). Cells were grown in suspension in alpha-MEM, supplemented with 10% FBS (HyClone) and 2 mM L-glutamine (Invitrogen), in a humidified incubator at 37 °C and 5% CO_2. Cells were passaged every 3−4 days.

3. Results and Discussion

3.1. Particle Synthesis and Characterization. Lanthanide-containing nanoparticles were synthesized by miniemulsion polymerization[13,14] of styrene in the presence of Ln ions bound to an organic ligand (tris-4,4,4-trifluoro-1-(2-naphthyl-1,3-butanedione)) (Chart 1). In most applications of the Eu and Tb derivatives, the ligand behaves as an antenna to absorb incident light and transfer the energy of it to the metal, which subsequently undergoes emission.[15,16] These complexes are electrically neutral and soluble in organic solvents. At the onset of the reaction, the complexes are fully soluble in the styrene phase. In miniemulsion polymerization, under ideal circumstances, each droplet corresponds to a nanoreactor undergoing bulk polymerization.[17] For example, Landfester et al.[18] have shown by a combination of conductivity, surface tension, and SANS experiments that a one-to-one copy from monomer droplets to polymer particles can be achieved. This type of ideal behavior is not always obtained.

This approach to the synthesis of polymer particles containing chelated lanthanides is similar to that reported recently by Ramirez et al.[19] These authors reported miniemulsion polymerization of butyl acrylate (BA) in water in which the BA droplets contained various lanthanides (Dy, Er, Eu, Gd, Ho, La, Pr, Yb) chelated with 2,2,6,6-tetramethyl-3,5-heptanedione. The key feature of the materials they obtained for specific BA/Ln mole ratios is an unprecedented spontaneous lamellar self-organization between the Ln complexes and the ester carbonyl group of the polymer. These particles had a relatively broad size distribution. We are more interested in particles with a narrower size distribution, which we imagine will have a similarly narrow distribution of lanthanide ions per particle.

In our reactions, the organic phase of the reaction mixture consisted of styrene, the lanthanide complex or mixture of complexes, and lauryl methacrylate (LM) to act as a polymerizable osmotic stabilizer against Ostwald ripening.[20−22] Most experiments employed potassium persulfate as the initiator, but in some experiments we tested 2,2′-azobis(2-methylbutyronitrile) (AMBN) as an oil-soluble initiator. The characteristics of the particles obtained are listed in Table 1. The polystyrene particles obtained had diameters ranging from 70 to 185 nm and relatively narrow size distributions. Repetition of individual reactions led to relatively small variability in particle diameters. Comparison of CV28 (no lanthanide) with CV90 and CV97 (mixed lanthanides, but the same amount of surfactant) shows some variability of particle size but no clear pattern. A bright field TEM image of the CV97 particles is presented in Figure 1.

(13) Antonietti, M.; Landfester, K. *Prog. Polym. Sci.* **2002**, *27* (4), 689−757.
(14) Schork, F. J.; Luo, Y. W.; Smulders, W.; Russum, J. P.; Butte, A.; Fontenot, K. *Adv. Polym. Sci.* **2005**, *175*, 129−255.
(15) Xiao, M.; Selvin, P. R. *J. Am. Chem. Soc.* **2001**, *123* (29), 7067−7073.
(16) Bassett, A. P.; Magennis, S. W.; Glover, P. B.; Lewis, D. J.; Spencer, N.; Parsons, S.; Williams, R. M.; De Cola, L.; Pikramenou, Z. *J. Am. Chem. Soc.* **2004**, *126* (30), 9413−9424.
(17) Landfester, K. *Macromol. Rapid Commun.* **2001**, *22* (12), 896−936.
(18) Landfester, K.; Bechthold, N.; Forster, S.; Antonietti, M. *Macromol. Rapid Commun.* **1999**, *20* (2), 81−84.
(19) Ramirez, L. P.; Antonietti, M.; Landfester, K. *Macromol. Chem. Phys.* **2006**, *207* (2), 160−165.
(20) Chern, C. S.; Liou, Y. C.; Chen, T. J. *Macromol. Chem. Phys.* **1998**, *199* (7), 1315−1322.
(21) Chern, C. S.; Liou, Y. C. *Polymer* **1999**, *40* (13), 3763−3772.
(22) Chern, C. S.; Chang, H. T. *Eur. Polym. J.* **2003**, *39* (7), 1421−1429.

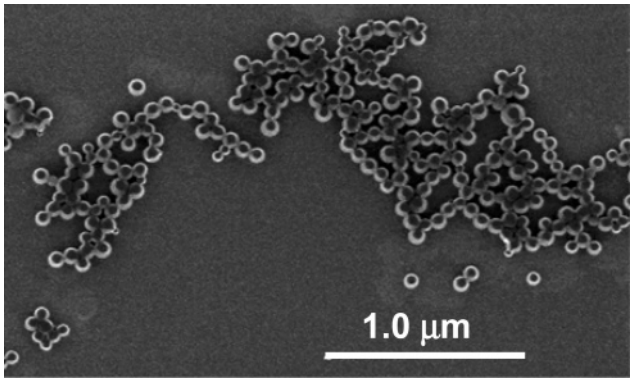

Figure 1. Bright-field TEM image of sample CV97 prepared with europium, terbium, holmium, praseodymium, and lanthanum complexes.

Particle contact seen in this image occurs upon drying. The particle diameters seen in the image correspond to that determined by DLS. There is no indication of particle aggregation in DLS measurements on any of the samples listed in Table 1.

Several authors[14,17,23] have examined the use of oil-soluble initiators in miniemulsion polymerization. One often finds that oil-soluble initiators produce larger particles in miniemulsion polymerization compared to reactions run with persulfate initiator. We attempted a number of reactions with AMBN (1 wt % based on styrene) as the initiator. Samples CV28 and CV70 (Eu) show the expected increase in particle diameter over those prepared with a persulfate initiator. One prominent difference between the two miniemulsion polymerization reactions carried out with AMBN as the initiator was the colloidal stability of the product. Metal-free CV28 proved to have excellent colloidal stability, comparable to that of particles prepared in the presence of persulfate. Stable particles could not be obtained by miniemulsion polymerization of styrene in the presence of the lanthanide complexes with AMBN as the initiator. Here it was necessary to modify the recipe to include a small amount of methacrylic acid (1 wt % based on styrene). In the former case, the surfactant itself provides colloidal stability without the surface $-OSO_3(-)$ groups that originate from the persulfate initiator. When the lanthanide chelate is present, one needs the additional contribution to colloidal stability provided by the $-COO(-)$ groups originating from the methacrylic acid co-monomer.

All of the samples listed in Table 1 showed good colloidal stability, although after several months a small amount of flocculation could be seen in some samples. This problem could be completely overcome by diluting the particles to ca. 2 wt % solids with $NaHCO_3$ (1 wt % in water) just after the polymerization. Samples treated this way have remained colloidally stable for more than a year.

The metal-ion-containing samples were less stable at low pH than the metal-free particles. Side-by-side experiments were carried out with CV90 ($d_m = 134$ nm, 2.5 wt % SDS based on styrene) and metal-free CV64 ($d_m = 104$ nm, 2 wt % SDS), both diluted to 3 wt % solids. By visual inspection, both were stable at pH 9. Upon addition of dilute HCl, the metal-containing particles flocculated at pH $\approx$ 5, whereas the metal-free particles remained stable until pH = 2.6. The origin of this effect is not completely clear but may be related to protonation of lanthanide complexes near the particle surfaces. The sulfate ($-OSO_3^-$) ions would be expected to remain dissociated over the pH range where the metal-containing particles lose their colloidal stability.

(23) Blythe, P. J.; Klein, A.; Phillips, J. A.; Sudol, E. D.; El-Aasser, M. S. *J. Polym. Sci., Part A: Polym. Chem.* **1999**, *37* (23), 4449−4457.

Table 2. ICP-AES and ICP-MS Analysis of CV97,[a] with the Results Reported as the Lanthanide Content of the Polystyrene Particles in (mg of Complex **2**)/(g of PS)

	mg of complex/g of PS							
method[b]	Ho	STD[c]	Pr	STD	Tb	STD	Eu	STD
				ICP-AES				
AR	3.01	0.04	2.12	0.05	2.54	0.04	5.38	0.08
direct	3.25	0.32	2.47	0.23	2.79	0.27	6.03	0.53
				ICP-MS				
AR	3.18	0.07	2.41	0.08	2.82	0.02	5.95	0.16
direct	3.13	0.1	2.26	0.14	2.77	0.20	7.06	0.31
mean	3.14		2.31		2.73		6.10	
ratio/Ho	1.0		0.74		0.87		1.94	

[a] Ion intensities were normalized to the intensity of 1.0 ppb Ir added to each sample. [b] AR: samples were digested with aqua regia prior to analysis; direct: samples were injected directly into the respective ICP-AES and ICP-MS instruments. [c] One standard deviation for triplicate samples subjected to similar sample preparation conditions. STD values for replicate analysis of the same sample are ca. 1% for ICP-MS and range from 5 to 9% for ICP-AES for samples close to the detection limit.

The metal ion content of sample CV97 was examined by both ICP-atomic emission spectroscopy (ICP-AES) and by ICP-mass spectroscopy (ICP-MS). Sample preparation for this type of analysis requires great care and can be a significant source of error. In Table 2, we compare the results for two different types of sample-handling protocols, predigestion of the samples with aqua regia (HNO_3 + HCl) and direct injection of the samples into the ionizing plasma of the ICP-AES and ICP-MS instruments. Prior to analysis, 1.00 ppb Ir was added to each sample. In the data analysis, signals for each of the elements were normalized to that of Ir, and then element abundances were converted to mg of complex per g of polystyrene using the predilution and predigestions particle content as determined by gravimetric analysis. For each analysis triplicate samples were examined in parallel. The mean values obtained by both techniques and by both sample preparation methods are similar. The data in the table exhibit a larger standard deviation for samples injected directly into the ICP source of both instruments than that for samples digested with aqua regia.

A "core−shell" particle sample (CV98) was prepared using an aliquot of CV97 as seed particles. The second-stage monomers consisted of styrene, divinyl benzene, and 1 wt % methacrylic acid based upon second-stage monomer. The *z*-averaged particle diameter increased from 90 nm for CV97 to 140 nm for CV98. Analysis of the metal ion content of CV98 gave ion ratios based on Holmium of Ho (1.0), Pr (0.62), Tb (0.84), and Eu (1.91), similar to the ratios found for CV97 (Table 2). The zeta potential for this particle (-28.6 ± 2.5) is smaller than that (-45.9 ± 3.6) of the CV97 precursor.

A curious feature of the data, which we do not yet understand, is that the metal ion content of the particles is smaller (CV74, CV97) than the metal complex content of the reaction mixture. Under visual inspection during and after the miniemulsion polymerization reaction, we did not detect any obvious precipitate. It is possible that a thin film of metal chelate formed on the reaction vessel and escaped notice. This is a point that merits further investigation in the future.

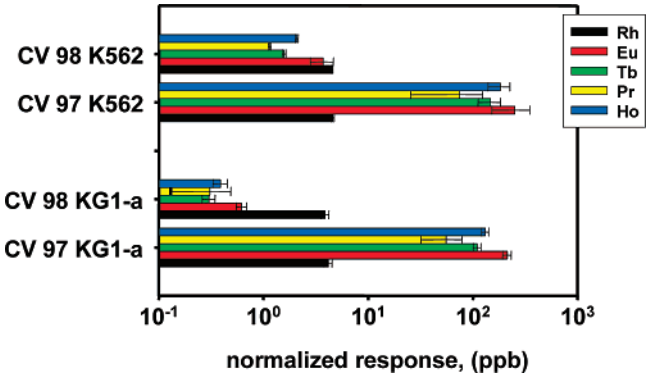

Figure 2. Nonspecific endocytosis of multielement coded polystyrene nanoparticles by human leukemia cells. The bars refer to raw intensity data for an individual isotope for each element, normalized by the intensity of 1.0 ppb Ir added to each sample prior to the analysis.

3.2. Tests of Endocytosis of the Metal-Containing Nanoparticles. Our intent in synthesizing the polymer nanoparticles (NPs) described above was to employ them as "element labels" for different cell types. The basic idea is that the particles would be taken up by the cells via nonspecific endocytosis and then later detected via ICP-MS. For this purpose, we chose three different human leukemia cell lines: KG-1a, an acute myelogenous leukemia; THP-1, an acute monocytic leukemia; and K562, a chronic myeloid leukemia.

Nonspecific endocytosis of the metal-containing polystyrene NPs was initially tested using the KG1a and K562 cell lines. NP preparations were diluted 1:10 in water and sterilized by pasteurization (24 h 70 °C). Two samples of multielement (Tb, Eu, Ho, Pr) NPs CV97 ($d = 90$ nm) and the carboxylated core−shell derivative CV98 ($d_z = 140$ nm) were added to cultures in amounts of $(0.5-1) \times 10^{11}$ particles/mL and incubated with cells for 5−48 h.

After incubation the cells were collected by low-speed centrifugation (1500 rpm, 5 min), washed twice with phosphate buffered saline (PBS) to remove free nanoparticles, and fixed with 3.7% formaldehyde/PBS for 30 min at room temperature. Following fixation, cells were washed once with PBS and stained with a Rh-containing metallointercalator.[24] The metallointercalator binds cellular DNA and was used as an internal normalizing agent across all samples. Stained cells with endocytosed beads were digested in concentrated HCl. Finally, the digests were combined with an equal volume of 1 ppb Ir/10%HCl internal standard and analyzed by volume ICP-MS. As negative controls, samples with growth media alone were incubated with beads and processed simultaneously with the samples containing cells and beads.

Results are presented in Figure 2. For both cell lines, the polystyrene CV97 NPs showed a greater level of endocytosis than the core−shell CV98 NPs. Note that the ^{103}Rh signal is constant for both NP preparations, indicating that the difference in levels of elements of endocytosed beads is not due to different cell numbers but rather to the affinity of cells either to the composition of the bead surface or the difference in particle size. Significantly, the elemental content of the beads inside cells remains the same as that in the initial bead preparations — more Eu, similar Ho and Tb, less Pr, thus "coding" the cells with a unique element identifier.

(24) Chow, C. S.; Barton, J. K. *Methods Enzymol.* **1992**, *212*, 219−242.

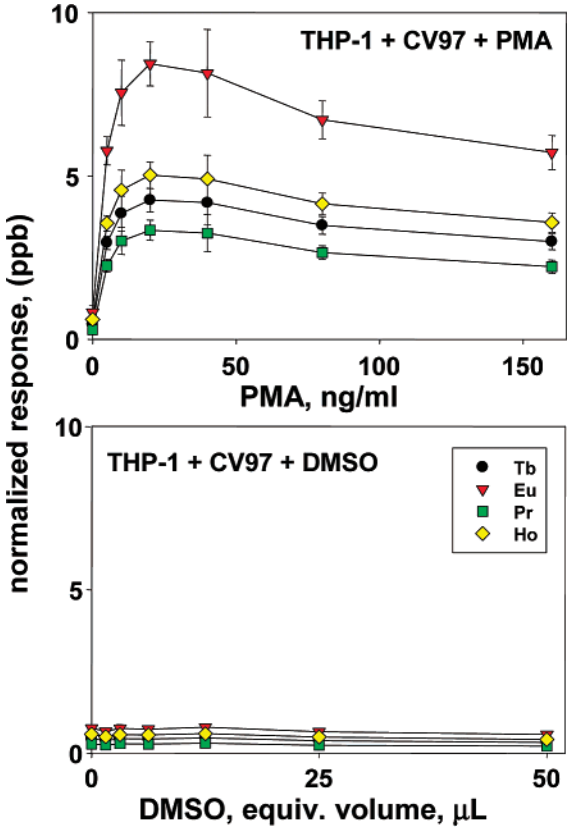

Figure 3. Adhesion assay for THP-1 cells treated with the differentiating agent PMA or with an equivalent volume of DMSO. The curves describing the elements detected, from top to bottom, are due to Eu, Ho, Tb, and Pr.

Next we investigated the potential of using metal-containing polystyrene nanoparticles for bioassays such as cell adhesion analysis. Growing THP-1 cells in suspension are known to respond to phorbol ester stimulation (PMA, phorbol 12-myristate 13-acetate) by differentiating into macrophage-like cells that readily attach to plastic substrates.[25] It is known that optimal concentrations of PMA result in the highest numbers of differentiated and attached cells.

This process was tested by seeding element "coded" cells into 96-well plates with different PMA concentrations. First, THP-1 cells were cultured in the presence of sterile CV97 (ca. 20 000 particles per cell) for 24 h. These cells were washed several times and plated in wells with increasing amounts of PMA (0−150 ng/mL) prepared as stock in DMSO and incubated for 2.5 days. For controls, plates were set up with different amounts of DMSO (equivalent volumes to PMA). After differentiation, the wells were washed several times with PBS, aspirated dry, and then filled with concentrated HCl. The digested material was combined with the Ir internal standard solution for ICP-MS volume analysis.

Figure 3 clearly shows that an elemental signature was generated only in the presence of PMA, indicating that cells became attached to the well bottom. PMA at 20 ng/mL induced the most differentiation and attachment, while concentrations above 150 ng/mL caused cell death and lower detected signal (dead cells are easily flushed from the wells during the washing step). Likewise, PMA below 20 ng/mL generated lower response

(25) Prieto, J.; Eklund, A.; Patarroyo, M. *Cell. Immunol.* **1994**, *156* (1), 191−211.

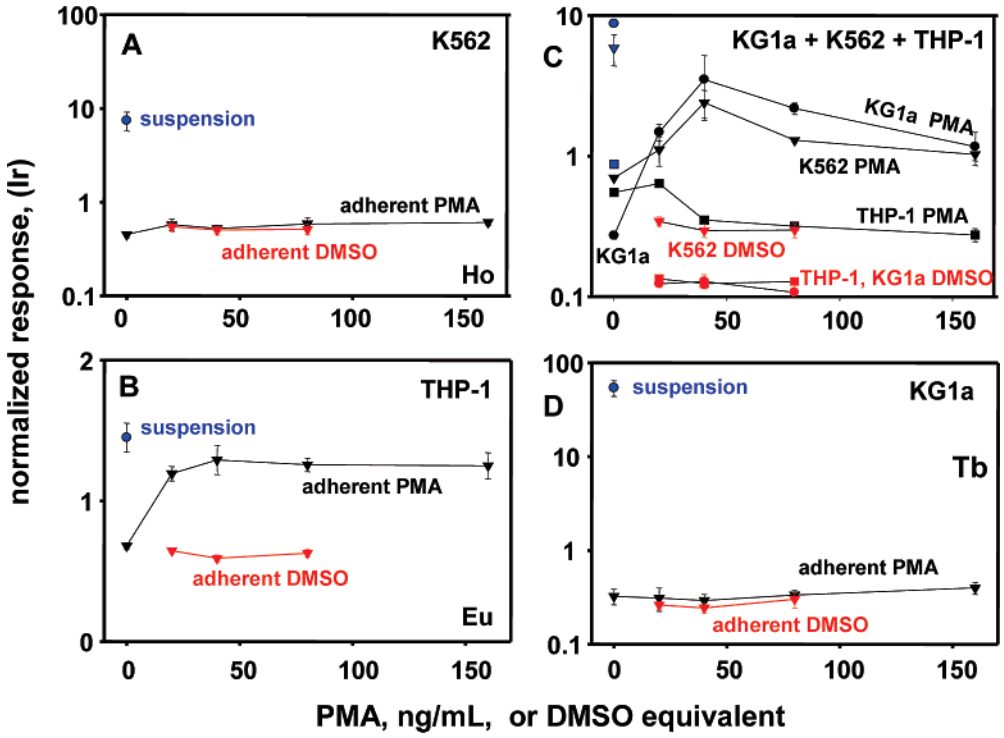

Figure 4. Influence of co-culture conditions on adhesion of cells individually marked with different element-coded polystyrene nanoparticles. The *x*-axis refers to the concentration of PMA added or the equivalent volume of DMSO. The *y*-axis is the ICP-MS signal intensity for each element normalized by that of the Ir internal standard in each sample. Graphs A, B, and D depict responses of single cell types (K562, THP-1, and KG1a, respectively) to stimulation (single cultures). Graph C shows the three tagged cell lines grown and stimulated in the same well (mixed culture). The blue symbols in A, B, and D refer to assays on cell suspensions. Black circles characterize KG1a; inverted triangles, K562; filled squares, THP-1. Red symbols in all graphs indicate measured responses in control DMSO-containing conditions. Individual particles contain about 10^3 lanthanide ions, either of a single element or a mixture of elements. These particles were internalized into three cell lines associated with human leukemia. Using an assay based upon ICP-MS detection, we could monitor quantitatively cell adhesion induced by cell differentiation of THP-1 cells in response to phorbol (PMA) ester stimulation.

due to less cell differentiation and attachment. DMSO had no effect on cell adhesion, and the normalized response remained very low for all volumes tested, since practically all cells remained in suspension and were efficiently washed away. As seen previously for CV97, the element composition of the cells with internalized beads was the same as that for the initial CV97 preparation.

Cells display various adhesion characteristics depending not only on the substrate but also on cell−cell interactions. The next set of experiments was designed to probe the attachment properties of the three different cell lines in mixed culture conditions. KG1-a cells are known to be insensitive to PMA stimulation and do not change their adhesion properties, while K562 cells respond to PMA by differentiating into megakaryocytes with a slightly increased ability to attach to tissue culture grade plastic.[26]

Single-element polystyrene NPs were used to uniquely mark individual cell types: KG1-a with CV45 (Tb); K562 with CV40 (Ho); and THP-1 with CV74 (Eu). Cells were incubated with beads under sterile conditions for 48 h, washed several times with PBS, and then plated into 96-well plates at 30 000 cells per well for individual cultures and at 10 000 cells per well of each cell type in mixed cultures (all the cell types in one well). Individual wells were filled with increasing concentrations of PMA or equivalent volumes of DMSO as described above. Cells were treated for 5 days. After incubation the cells were washed and digested in acid. Cells from wells that had no PMA or DMSO and did not adhere to the plastic were collected by aspiration, washed, digested in HCl, and used as an indication of the initial seeding of cells. These results are presented in Figure 4. As was expected, KG1-a cells alone did not attach to the plastic, and the response is similar for PMA and DMSO (Figure 4D). The blue circle at $x = 0$ in this figure indicates that, initially, the cells in suspension contained a high amount of Tb. The high Tb content of these cells indicates that endocytosis was as effective for these somewhat larger particles (CV45, see Table 1) prepared with an oil-soluble initiator and 1 wt % methacrylic acid in the recipe as for the other particles prepared with persulfate as the initiator.

Likewise, K562 cells alone have a similar profile after both treatments (Figure 4A) and a high Ho content in the initial culture. A different response is observed for THP-1 (Figure 4B). Here increasing PMA concentrations (but not DMSO) cause the cells to become macrophage-like and attach to the plate. This response is similar to that seen with the CV97-coded THP-1 cells in Figure 3. The response from the suspended cells when no PMA was added is not very different from that of the cultures treated with 20−50 ng/mL PMA, indicating that under these conditions practically all of the seeded cells differentiated and adhered to the plastic.

A very different result is seen when all three cell types are mixed together and treated with PMS. As seen in Figure 4C, under these conditions, KG-1a and K562 cells now become adherent. This effect can be explained by the cellular interactions that take place between the differentiated THP-1 cells that adhere to the plastic substrate and the KG1-a and K562

(26) Herrera, R.; Hubbell, S.; Decker, S.; Petruzzelli, L. *Exp. Cell Res.* **1998**, *238* (2), 407−414.

cells suspended in the solution. These two cell types now adhere to THP-1 cells or to its extracellular matrix rather than to the plastic. Moreover, stimulated monocytic cells may start to secrete interleukine, cytokines, and TNF-a which would in turn influence integrin expression on PMA nonresponsive cells.[27]

Further investigation into these interactions is necessary to understand intercellular communication in mixed co-cultures. Encoding cells with unique-element polymer nanoparticles may make this possible.

4. Summary

We have described the synthesis and characterization of element-encoded polystyrene nanoparticles with diameters on the order of 100 nm and a narrow size distribution. Individual particles contain ca. 10^3 chelated lanthanide ions, either of a single element or a mixture of elements. These particles were effectively internalized by nonspecific endocytosis into three cell lines associated with human leukemia. Using an assay based upon ICP-MS detection, we could quantitatively monitor cell adhesion induced by cell differentiation of growing THP-1 cells in suspension in response to phorbol (PMA) ester stimulation.

Acknowledgment. The authors thank NSERC Canada, Genome Canada and the Ontario Genomics Institute for their support of this research.

JA073970W

(27) Bhatia, R.; Wayner, E. A.; Mcglave, P. B.; Verfaillie, C. M. *J. Clin. Invest.* **1994**, *94* (1), 384−391.